dria [50 μg of mitochondrial proteins in 50 μl of 250 mM sucrose, 10 mM Hepes, 1 mM ATP, 5 mM succinate, 0.08 mM ADP, 2 mM $K_2HPO_4$, 32 mM KCl, and 0.8 mM $MgCl_2$ (pH 7.4)] for the indicated times at 25°C. For the dose response experiment, indicated amounts of complex in 1 μl of wheat germ extract were incubated with isolated liver mitochondria [50 μg of mitochondrial proteins in 50 μl of 150 mM KC1, 10 mM tris, 1 mM $K_2HPO_4$, 5 mM glutamate, 2.5 mM malate, and 0.01 mM EGTA (pH 7.4)] for 45 min at 25°C.

29. Wt and G60A p22 BID with a COOH-terminal GFP fusion were cloned into the Bam HI and Eco RI sites of pBabe puro vector. The recombinant viruses were produced with a VSV-G packaging cell line (*25*). MCF7 cells were infected with the viruses and selected in Dulbecco's modified Eagle's medium containing puromycin (1.5 μg/ml). The puromycin-resistant cells were used for protein immunoblot analysis, viability, and confocal microscopy.

30. We thank R. C. Mulligan, E. S. Alnemri, V. M. Dixit, and R. J. Collier for providing the cell lines and reagents used in these experiments and E. D. Smith for assistance in preparing the manuscript. J.Z. is supported by a Howard Temin Award from the National Cancer Institute (K01 CA82231) and by NIH training grant T32 CA72320-01A1. Supported by NIH grant CA50239-13.

17 August 2000; accepted 26 October 2000

# Requirement of the RNA Editing Deaminase ADAR1 Gene for Embryonic Erythropoiesis

**Q. Wang, J. Khillan, P. Gadue, K. Nishikura***

**The members of the ADAR (adenosine deaminase acting on RNA) gene family are involved in site-selective RNA editing that changes adenosine residues of target substrate RNAs to inosine. Analysis of staged chimeric mouse embryos with a high contribution from embryonic stem cells with a functional null allele for ADAR1 revealed a heterozygous embryonic-lethal phenotype. Most ADAR1$^{+/-}$ chimeric embryos died before embryonic day 14 with defects in the hematopoietic system. Our results suggest the importance of regulated levels of ADAR1 expression, which is critical for embryonic erythropoiesis in the liver.**

The adenosine-to-inosine (A-to-I) RNA editing by ADAR (*1*) results in the creation of alternative splicing sites (*2*) or alteration of codons and, thus, leads to functional changes in proteins. Target genes for ADAR include ionotropic glutamate receptors (GluRs) (*3, 4*) and serotonin receptor 2C subtype (5-$HT_{2C}$R) (*5*) in the brain and hepatitis delta virus antigen (*6*) in the liver. Three separate ADAR gene family members (ADAR1 to ADAR3) that display substantial differences in their substrate and editing site selectivity (*7–13*) have been identified in humans and rodents. Both ADAR1 and ADAR2 are expressed in many tissues (*7–9, 13*), whereas ADAR3 is expressed only in the brain (*10, 14*). In view of the ubiquitous expression of ADAR1 and ADAR2, it has been predicted that A-to-I RNA editing is likely to extend to additional target genes yet to be identified (*15*).

Using a targeting vector construct in which the two exons, E12 and E13, corresponding to a part of the catalytic domain (*16*), were replaced with a PGK-neo gene, we created a mutation of the mouse ADAR1 gene in early passage (P13) R1 (*17*) embryonic stem (ES) cells (*18*). Four separate ADAR1$^{+/-}$ ES cell clones identified did not exhibit any obvious alteration in their morphology or growth. The level of functional ADAR1 mRNA (*19*) derived from the remaining ADAR1$^{+}$ allele in the targeted ES cells was reduced to about half of that in ADAR1$^{+/+}$ R1 cells as expected (Fig. 1A). We attempted to prepare ADAR1 mutant mouse lines with the nonfunctional ADAR1$^{-}$ gene locus by coaggregating the ES cell lines with blastocysts derived from FVB/N albino donor mice (*17*). However, we encountered difficulties in obtaining chimeric mice that could vertically transmit the ADAR1$^{-}$ allele. The very limited number of mice that were born alive with a normal appearance were later found to be either nonchimeric or chimeras with a very limited contribution of ADAR1$^{+/-}$ cells (Table 1). These results led us to suspect embryonic lethality in ADAR1$^{+/-}$ chimeric mice. The double-stranded RNA (dsRNA) binding domains located from E2 to E7 (*16*) were not altered during targeting. Thus, a COOH-terminal–truncated ADAR1 protein without its deaminase domain, but capable of binding to substrate RNAs, could be generated from the ADAR1$^{-}$ allele (*18*). Potentially such aberrant ADAR1 proteins, if translated, might compete with and thus inhibit the activity of the wild-type enzyme derived from the ADAR1$^{+}$ allele (*10*). However, Western blot analysis with a specific monoclonal antibody (mAb) raised against the region E2 to E8, detected only wild-type ADAR1 proteins of the expected size in the ADAR1$^{+/-}$ ES cells at reduced level, 50 to 60% of that in ADAR1$^{+/+}$ R1 ES cells (Fig. 1B). This result makes it very unlikely that dominant-negative inhibition by a COOH-terminal–truncated ADAR1 protein is the mechanism for the observed heterozygous-lethal phenotype.

Embryonic teratomas derived from ADAR1$^{+/-}$ ES cells were next examined for potential deficiencies in their ability to differentiate. All tumors contained a variety of differentiated and undifferentiated tissues, but with an abundance of cells of neuronal origin (70 to ~90%). No obvious histological difference was found among tumors derived from ADAR1$^{+/+}$ (R1) or ADAR1$^{+/-}$ (cl 52 and cl 119) ES cells. Because these tumors were clonal in nature and thus homogeneous for ADAR1 alleles, total RNA was extracted and tested for several known A-to-I editing sites of GluR-B, GluR5, and GluR6 subunits and 5-$HT_{2C}$R RNA. In the ADAR1$^{+/-}$ tumors a significant decrease (20 to 40%) in editing efficiency was found at the R/G site of GluR-B, the Q/R site of GluR5, and the A and B sites of 5-$HT_{2C}$R RNA (Table 2). In vitro editing of these sites by ADAR1 has been previously demonstrated (*5, 7–12, 20*). In contrast, the editing efficiency of the Q/R site of GluR-B and the D site of 5-$HT_{2C}$R, previously shown to be edited in vitro by ADAR2, occurred at the same level in tumors derived from ADAR1$^{+/-}$ ES cells and R1 cells. Thus, inactivation of even a single copy of ADAR1 gene has significant effects on the overall A-to-I RNA editing efficiency of ADAR1 target genes. A similar decline in the extent of editing at several known sites has been reported also for ADAR2$^{+/-}$ heterozygote mice (*21*). These known sites, as well as currently unidentified ADAR1 target sites, are likely to be underedited in ADAR1$^{+/-}$ chimeric embryos (see below).

A series of experiments were next conducted in which the staged chimeric embryos were recovered at different time points, from embryonic day 9.5 (E9.5) to E18.5 (Table 1). Although ADAR1$^{+/-}$ chimeric embryos, at least up to stage E11.5, exhibited no obvious abnormality, no live chimeric embryo beyond E14.5 with a high degree of contribution by ADAR1$^{+/-}$ cells was recovered (Table 1). A small number of chimeric embryos, in which the contribution of ADAR1$^{+/-}$ cells was >90%, survived to E12.5 and E13.5 (Table 1). ADAR1 functional mRNA derived from the ADAR1$^{+}$ allele, though at substantially reduced levels (40 to 50%), was detected in these surviving chimeric embryos (Fig. 1A). Thus, the heterozygous embryonic lethal phenotype of ADAR1$^{+/-}$ chimeric embryos appears not due to a gene imprinting mechanism. The tight dose-dependent, heterozy-

Wistar Institute, Philadelphia, PA 19104, USA.

*To whom correspondence should be addressed. E-mail: kazuko@wistar.upenn.edu

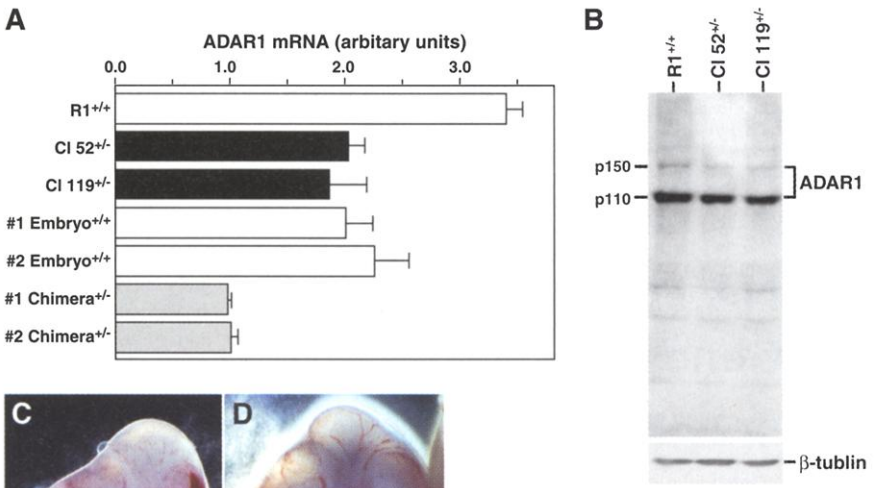


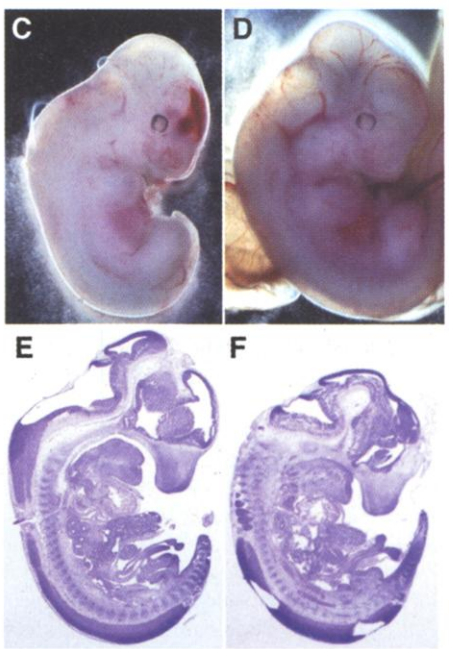


**Fig. 1.** Detection of ADAR1 mRNA and protein in ADAR1$^{+/-}$ ES cells and chimeric embryos. (**A**) Detection of the functional ADAR1 mRNA by quantitative RT-PCR. Results are presented as means ± SE (error bars) of three independent measurements ($n$ = 3). The contribution of ADAR1$^{+/-}$ ES cells in two E12.5 chimeric embryos examined was more than 90%. The ADAR1 mRNA levels were reduced to 62% and 54% in ADAR1$^{+/-}$ cl 52 and cl 119, respectively, in comparison to ADAR1$^{+/+}$ R1 ES cells. The ADAR1 mRNA levels detected in E12.5 chimeric embryos were reduced to 40 to 50% of that in control embryos. (**B**) The detection of ADAR1 proteins in ES cells. A mouse mAb 15.8.6, raised against the middle region (E2 to E8) of ADAR1 protein (*29*), was used for Western blotting analysis of ES cells. The same blot was rehybridized with anti–β-tubulin mAb T-5293 (Sigma, St. Louis, Missouri) for normalization. The two functional ADAR1 proteins (p150 and p110) were described previously (*30*). (**C** to **F**) Gross appearance of chimeric embryos. Live ADAR1$^{+/-}$ chimeric embryos were recovered at E12.5 (C and E) and E13.5 (D and F). Histology sections stained with hematoxylin (E and F) revealed no gross abnormality for these chimeric embryos (>90% contribution).

gous, embryonic-lethal phenotype observed with our ADAR1$^{+/-}$ embryos is unusual, but not unprecedented (*22*).

The gross appearance and overall organogenesis of the live ADAR1$^{+/-}$ chimeric embryos appeared to be normal (Fig. 1, C to F). On close examination of these chimeric embryos, however, major defects in erythropoiesis were found. Around E12, the major site of hematopoiesis changes from the yolk sac to the liver (*23*). Erythrocytes synthesized in the yolk sac before E12 remain nucleated, whereas those generated in the liver mature and lose their nuclei as development progresses. In normally developing embryos, the fraction of nucleated erythrocytes in peripheral blood thus rapidly decreases from 100% at E10.5 to 75% at E12.5, 45% at E13.5 (Fig. 2A), and 13% at E14.5. All erythrocytes become enucleated by E16.5 (Fig. 2C). In contrast, peripheral blood erythrocytes of chimeric embryos at E12.5 and E13.5 stages with high contribution of ADAR1$^{+/-}$ cells (>90%) remained for the most part completely nucleated (Fig. 2C). In addition, substantial numbers of the nucleated erythrocytes appeared to be undergoing mitosis or had an open chromatin structure (Fig. 2B), features that were not observed with age-matched control embryos (Fig. 2A).

Although our results indicate abnormal proliferation and/or differentiation of blood cells, at present we do not know whether the problems are caused by defects in the hepatic environment, which in turn affect erythropoiesis, or in the erythroid precursors themselves. Similar embryonic-lethal phenotypes stemming from defects in hepatic erythropoiesis have been reported for Rb$^{-/-}$ mouse embryos, probably as a result of the intrinsic and mitogenic changes in erythroblasts (*24*). Although overall liver architecture revealed by histological examination was not signifi-

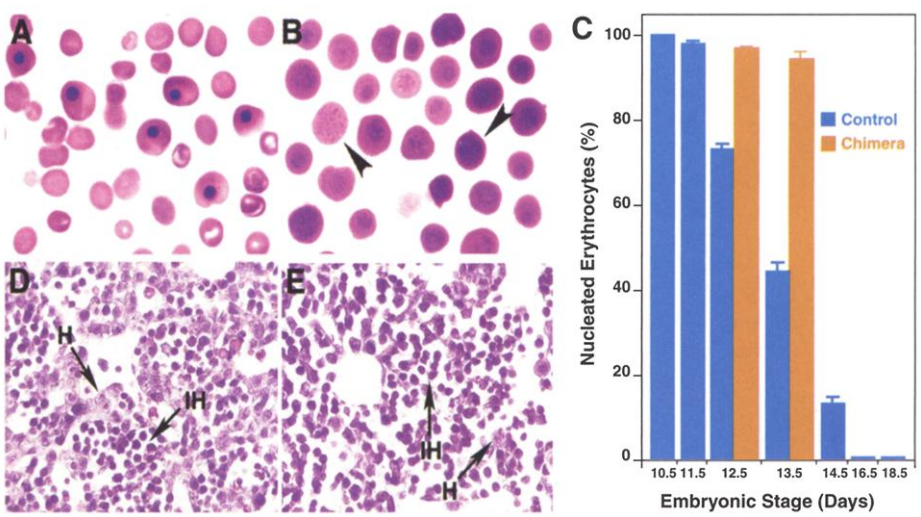


**Fig. 2.** Histological analysis of the hematopoietic system and liver. (**A** and **B**) Embryonic peripheral blood was collected from the umbilical vein and artery and stained with Wright-Giemsa (magnification, ×160). The wild-type ADAR1$^{+/+}$ embryos at E13.5 (A) and the chimeric ADAR1$^{+/-}$ embryos (>90% contribution) at E13.5 (B). (Arrowheads indicate a representative cell in mitosis and a cell with an open chromatin structure.) (**C**) The fraction of the nucleated erythrocytes of ADAR1$^{+/+}$ control embryos (blue bar) at different stages and E12.5 and E13.5 chimeric embryos (orange bar). More than 200 erythrocytes each from three separate blood smear slides were scored. Bars represent the SEs ($n$ = 3). (**D** and **E**) Liver sections were stained with hematoxylin and eosin (magnification ×100). Numerous islands of hematopoietic cells (IH, indicated by arrows) filling the sinusoids of the liver were found both in the wild-type (D) and ADAR1$^{+/-}$ chimeric embryos (E) at E12.5. A smaller number of hepatocytes (H, indicated by arrows) are detected in the chimera than in the control embryo.

cantly impaired, the livers of E12.5 and E13.5 ADAR1$^{+/-}$ chimeric embryos displayed a lacy appearance that reflected a lower hepatocyte cell density than in control embryos (Fig. 2, D and E). However, the numbers of hematopoietic cells or islands present in the liver are very similar between chimeric and wild-type embryos (Fig. 2, D and E). This is in contrast to the total lack of the hepatic hematopoiesis reported for c-*myb*$^{-/-}$ mouse embryos (*25*).

Although the ADAR1 mRNA is detected in many adult human and rodent tissues (*13*), immunohistochemistry analysis has revealed that the ADAR1 expression progressively increases in wild-type ADAR1$^{+/+}$ mouse embryos around the mid to late stage of the development (Fig. 3, A to C). ADAR1 protein expression was barely detectable in wild-type embryos at E10.5 (Fig. 3A). At E11.5 and E12.5 stages, however, several tissues, including liver, begin to express ADAR1 proteins, and around E13 to E14, hepatic expression of ADAR1 increases substantially (Fig. 3, C and E). In contrast, the ADAR1 expression levels in chimeric embryos at E12.5 and E13.5 (Fig. 3, F and G) are lower than those of wild-type embryos (Fig. 3, D and E), especially at E13.5 stage. Our results suggest a requirement of regulated increase in the ADAR1 expression in liver at E12 and E13 stages. Failure to increase ADAR1 may result in underediting of the RNA of currently unknown target genes, which in turn affects proliferation and/or differentiation of erythrocytes. An absence of mature erythrocytes would lead to tissue hypoxia and the eventual death of the embryo (*23*).

Our results are in contrast to the less severe phenotype of viable ADAR2$^{-/-}$ mice reported recently (*21*). The difference observed between ADAR1 and ADAR2 mutations is likely to reflect the different repertoires of genes targeted for RNA editing by these two enzymes. As a precedent for the unexpectedly dramatic consequence of A-to-I

**Table 1.** Quantitative analysis of ES cell contribution in ADAR1$^{+/-}$ chimeras. Control (R1) and two separate ES cell clones (cl 52 and cl 119) were used for preparation of chimeras. The extent of the chimerism and the contribution of ADAR1$^{+/-}$ ES cells were examined by glucose phosphate isomerase (GPI) isoenzyme analysis (*27*) followed by direct densitometric scanning of GPI bands separated on cellulose acetates plates. The GPI isotype of R1 and ADAR1$^{+/-}$ ES cell lines is GPI-1A, whereas FVB/N host mice express GPI-1B (*27*). The dead chimeric embryos recovered at late stages were partly degenerated, and the embryos may have died at an earlier stage than listed.

| Blastocysts transferred | Age analyzed | Embryos or pups recovered (%)* | Chimeras recovered (%)† | ES cell contribution in chimeras | | |
|---|---|---|---|---|---|---|
| | | | | 0–30% | 30–60% | 60–100% |
| R1 (ADAR1$^{+/+}$) | | | | | | |
| 59 | >P1 | 20 (34) | 12 (60) | | 3 | 9 |
| cl 52 and cl 119 (ADAR1$^{+/-}$) | | | | | | |
| 82 | >P1 | 14 (17) | 3 (21) | 3 | | |
| 63 | E18.5 | 19 (30) | 5 (26) | 2 | 1 | 2 dead |
| 51 | E16.5 | 13 (25) | 6 (46) | 2 | 3 | 1 dead |
| 44 | E14.5 | 14 (32) | 10 (31) | 5 | 3 | 2 dead |
| 36 | E13.5 | 13 (36) | 7 (54) | | 2 | 5 (2 dead) |
| 63 | E12.5 | 21 (33) | 14 (67) | 4 | 3 (1 dead) | 7 (2 dead) |
| 10 | E11.5 | 3 (30) | 3 (100) | | | 3 |
| 16 | E9.5 | 9 (56) | 5 (56) | | 1 | 4 |

*Embryos recovered as a percentage of blastocysts tranferred. †Chimeric embryos recovered as a percentage of total embryos recovered.

**Table 2.** Altered RNA editing in ADAR1$^{+/-}$ teratomas. Five female Balb/c SCID mice (Wistar Institute, Philadelphia, Pennsylvania ) 6 weeks old were injected subcutaneously with $1 \times 10^7$ ES cells (R1, cl 52, or cl 119) in a volume of 0.1 ml (*22*). After 4 weeks, teratomas were recovered and processed for RNA extraction. Editing of GluR RNAs was estimated by RNA editing–sensitive restriction-site analysis of $^{32}$P-labeled RT-PCR products as described (*28*) except for the usage of murine GluR-specific primers. Quantitation of editing efficiency at four major sites of 5-HT$_{2C}$R was done by dideoxy oligonucleotide primer extension analysis of RT-PCR products (*10*). The values given as mean ± SE (five separate tumors, $n = 5$) indicate the percentage of editing at the different editing sites examined.

| Editing site | ADAR1$^{+/+}$ (R1) | ADAR1$^{+/-}$ (cl 52) | ADAR1$^{+/-}$ (cl 119) |
|---|---|---|---|
| GluR-B | | | |
| Q/R | 100 | 100 | 100 |
| R/G | 62 ± 4 | 39 ± 5 | 36 ± 6 |
| GluR5 | | | |
| Q/R | 65 ± 3 | 44 ± 7 | 41 ± 2 |
| GluR6 | | | |
| Q/R | 86 ± 3 | 77 ± 5 | 85 ± 2 |
| 5-HT$_{2C}$R | | | |
| A | 75 ± 2 | 64 ± 2 | 61 ± 4 |
| B | 54 ± 5 | 49 ± 6 | 38 ± 5 |
| C | 29 ± 3 | 27 ± 2 | 24 ± 6 |
| D | 37 ± 5 | 42 ± 4 | 39 ± 5 |

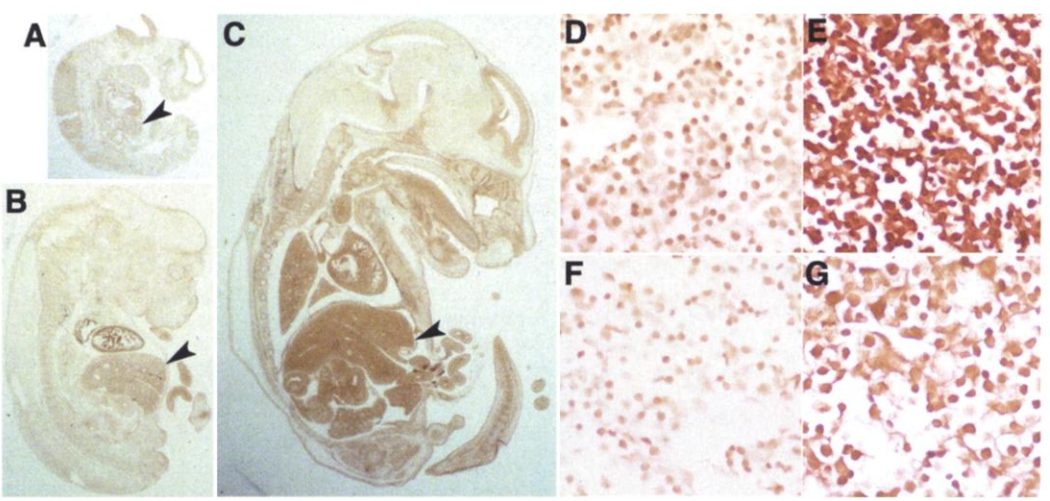


**Fig. 3.** Immunohistochemical analysis of mouse embryos for ADAR1 protein expression. Nonspecific staining of mouse embryo paraffin-embedded sections by mAb 15.8.6 was blocked by the M.O.M. Kit (Vector, Burlingame, California). Primary antibody was detected by the horseradish peroxidase (HRP)–labeled Biotin-Streptavidin Kit (KPL, Gaithersburg, Maryland). Wild-type (ADAR1$^{+/+}$) embryos at E10.5 (**A**), E12.5 (**B**), and E14.5 (**C**) stage. Arrowheads indicate embryonic livers. High-magnification view (×160) of liver sections derived from wild-type ADAR1$^{+/+}$ embryos, E12.5 (**D**) and E13.5 (**E**), and chimeric ADAR1$^{+/-}$ embryos (>90% contribution), E12.5 (**F**) and E13.5 (**G**).

RNA underediting, epileptic death of mutant mouse lines caused solely by a modest decrease (20 to 40%) in the editing efficiency of a single site (GluR-B Q/R site) has been reported (*26*). Our current efforts are focused on identification of the ADAR1 target genes critical for development.


**References and Notes**

1. B. L. Bass *et al.*, *RNA* **3**, 947 (1997).
2. S. M. Rueter, T. R. Dawson, R. B. Emeson, *Nature* **399**, 75 (1999).
3. M. Higuchi *et al.*, *Cell* **75**, 1361 (1993).
4. H. Lomeli *et al.*, *Science* **266**, 1709 (1994).
5. C. M. Burns *et al.*, *Nature* **387**, 303 (1997).
6. A. G. Polson, B. L. Bass, J. L. Casey, *Nature* **380**, 454 (1996).
7. T. Melcher *et al.*, *Nature* **379**, 460 (1996).
8. F. Lai, C.-X. Chen, K. C. Carter, K. Nishikura, *Mol. Cell. Biol.* **17**, 2413 (1997).
9. A. Gerber, M. A. O'Connell, W. Keller, *RNA* **3**, 453 (1997).
10. C.-X. Chen *et al.*, *RNA* **6**, 755 (2000).
11. G. A. Dabiri, F. Lai, R. A. Drakas, K. Nishikura, *EMBO J.* **15**, 34 (1996).
12. Q. Wang *et al.*, *J. Neurochem.* **74**, 1290 (2000).
13. U. Kim *et al.*, *Proc. Natl. Acad. Sci. U.S.A.* **91**, 11457 (1994).
14. T. Melcher *et al.*, *J. Biol. Chem.* **271**, 31795 (1996).
15. M. S. Paul, B. L. Bass, *EMBO J.* **17**, 1120 (1998).
16. Y. Wang, Y. Zeng, J. M. Murray, Nishikura, *J. Mol. Biol.* **254**, 184 (1995).
17. A. Nagy *et al.*, *Proc. Natl. Acad. Sci. U.S.A.* **90**, 8424 (1993).
18. Supplementary material is available at *Science* Online at www.sciencemag.org/cgi/content/full/290/5497/1765/DC1.
19. The functional ADAR1 mRNA levels were determined with 0.5 μg of total RNA extracted from ES cells or whole embryos with LightCycler-RNA Amplification Kit and LightCycler (Roche Molecular Biochemicals, Indianapolis, IN). To control for variations in sample preparation and RNA concentration measurement, all reverse transcriptase–polymerase chain reaction (RT-PCR) reactions were normalized for hypoxanthine phosphoribosyltransferase (HPRT) expression as described [P. Gadue *et al.*, *J. Exp. Med.* **190**, 1189 (1999)]. The following primers were used for detection of ADAR1 mRNA levels: MADAR1 sense, CCTGTGGAGTCCAGTGAT; and MADAR1 antisense, TGACAATAAAGGGATAGCGT. Because the region amplified corresponds to E12 and E13, which were deleted during targeting, the ADAR1 mRNA detected must be derived from the nontargeted ADAR1$^+$ allele.
20. A. Herb, M. Higuchi, R. Sprengel, P. H. Seeburg, *Proc. Natl. Acad. Sci. U.S.A.* **93**, 1875 (1996).
21. M. Higuchi *et al.*, *Nature* **406**, 78 (2000).
22. N. Ferrara *et al.*, *Nature* **380**, 439 (1996).
23. E. S. Russell, *Adv. Genet.* **20**, 357 (1979).
24. N. Hu, M. L. Gulley, J. T. Kung, E. Y.-H. P. Lee, *Cancer Res.* **57**, 4123 (1997).
25. M. L. Mucenski *et al.*, *Cell* **65**, 677 (1991).
26. D. Feldmeyer *et al.*, *Nature Neurosci.* **2**, 57 (1999).
27. A. L. Joyner, Ed., *Gene Targeting—a Practical Approach* (IRL, Oxford Univ. Press, Oxford, 1993).
28. F. Lai, C.-X. Chen, V. M.-Y. Lee, K. Nishikura, *J. Neurochem.* **69**, 43 (1997).
29. O. Railskin, D.-S. C. Cho, J. Sperling, K. Nishikura, R. Sperling, unpublished results.
30. J. B. Patterson, C. E. Samuel, *Mol. Cell. Biol.* **15**, 5376 (1995).



31. We thank A. Nagy for R1 cells; J. Wheeler, J. Golden, H. S. Baldwin, and K. Zarett for examination of histology sections and D. Solter and J. M. Murray for reading and comments on this manuscript. This work was supported by grants from NIH, the Human Frontier Program Organization, and the Doris Duke Charitable Foundation.

3 August 2000; accepted 17 October 2000


REPORTS

# Down-Regulation of the Macrophage Lineage Through Interaction with OX2 (CD200)


**Robert M. Hoek,[1] Sigrid R. Ruuls,[1] Craig A. Murphy,[1] Gavin J. Wright,[2] Ruth Goddard,[2] Sandra M. Zurawski,[1] Bianca Blom,[1] Margit E. Homola,[1] Wolfgang J. Streit,[3] Marion H. Brown,[2] A. Neil Barclay,[2] Jonathon D. Sedgwick[1]***



**OX2 (CD200) is a broadly expressed membrane glycoprotein, shown here to be important for regulation of the macrophage lineage. In mice lacking CD200, macrophage lineage cells, including brain microglia, exhibited an activated phenotype and were more numerous. Upon facial nerve transection, damaged CD200-deficient neurons elicited an accelerated microglial response. Lack of CD200 resulted in a more rapid onset of experimental autoimmune encephalomyelitis (EAE). Outside the brain, disruption of CD200-CD200 receptor interaction precipitated susceptibility to collagen-induced arthritis (CIA) in mice normally resistant to this disease. Thus, in diverse tissues OX2 delivers an inhibitory signal for the macrophage lineage.**


OX2 (now CD200) (*1*) is expressed in diverse cell types and tissues, ranging from splenic B lymphocytes to central nervous system (CNS) neurons (*2*, *3*). It shares a two-immunoglobulin (Ig)-domain arrangement with molecules involved in T lymphocyte regulation (*4*), including CD2, 2B4, CD80, and CD86, and is genetically linked to the latter two (*5*). However, the broad expression pattern of CD200 and the finding that CD200-receptor (CD200R) expression is restricted to myeloid lineage cells (*6*, *7*) points instead to a role for CD200 in regulation of myeloid-derived cells.

To investigate CD200 function, we generated CD200 gene-targeted mice using C57BL/6 embryonic stem cells (*8–10*). Heterozygous (+/−) and homozygous (−/−) mice were grossly normal in appearance, bred normally, exhibited a normal life-span, and showed no obvious behavioral changes. Immunohistochemical (*11*) and flow cytometric (*12*) staining with a new monoclonal antibody to murine CD200 (mCD200, OX90) (*13*) showed expression on neurons in the CNS and on B cells, follicular dendritic cells (FDCs), and endothelium in splenic tissue in wild-type (+/+) mice, but not −/− mice (*2*, *3*) (Fig. 1). By contrast, splenic myeloid-lineage cells of +/+ mice (CD11b$^+$ macrophages and granulocytes) expressed no CD200 (Fig. 1). Levels of expression of B220, CD4, CD8, and CD11b were comparable between CD200−/− and +/+ mice (Fig. 1B). In the spleen of CD200$^{-/-}$ mice, changes were detected only in the CD11b$^+$ population, which doubled in size (Fig. 1B and Table 1), with both F4/80$^{lo}$-GR1$^{hi}$ granulocytes and F4/80$^{hi}$-GR1$^{lo}$ mature macrophages expanded significantly (Table 1). Thus, the absence of CD200 resulted in an increase in cells that do not express CD200, but rather its receptor (*7*).

The increased CD11b$^+$ population in CD200$^{-/-}$ mice was reflected in splenic red pulp enlargement, visualized by a larger surface area staining with F4/80 (Fig. 2, A and B). MOMA-1$^+$ metallophilic marginal zone macrophages were transformed from a thin, single cell layer (*14*) to a thick, multicell layer (Fig. 2, C and D). Higher expression of the ITAM-containing intracellular activation protein DAP12, shown to be an essential component of normal myeloid cell function (*15*), indicated that macrophage populations were activated in CD200$^{-/-}$ mice, particularly in the marginal zone (Fig. 2, E and F). Dendritic cells (DCs), which are CD200R$^+$ (*7*) and reside in the T cell area of the white pulp, also showed increased activation.

CD200$^{-/-}$ mice had slightly enlarged lymph nodes, especially the mesenteric lymph nodes (MLNs), changing from interconnected but well-defined spherical structures in +/+ mice (Fig. 2G) to a tubular formation, without clear demarcation between nodes (Fig. 2H). In addition, lymph node macrophages were expanded and activated substantially in CD200$^{-/-}$ mice (Fig. 2H).

Because microglia, the resident CNS macrophage (*16*, *17*), are CD200R$^+$ (*7*), neurons could in principle interact with and regulate microglia function through their expression of CD200 (Fig. 1A) (*3*). In healthy +/+ mice, microglia are quiescent cells expressing mole-


[1]DNAX Research Institute of Molecular and Cellular Biology, 901 California Avenue, Palo Alto, CA 94304, USA. [2]Sir William Dunn School of Pathology, University of Oxford, Oxford OX1 3RE, UK. [3]Department of Neuroscience, College of Medicine and Brain Institute, University of Florida, Gainsville, FL 32610, USA.

*To whom correspondence should be addressed. E-mail: jon.sedgwick@dnax.org